A Broadband Planar Magic-T Using Microstrip–Slotline Transitions

Kongpop U-yen, *Member, IEEE*, Edward J. Wollack, *Senior Member, IEEE*, John Papapolymerou, *Senior Member, IEEE*, and Joy Laskar, *Fellow, IEEE*

***Abstract*—The improved version of a broadband planar magic-T using microstrip–slotline transitions is presented. The design implements a small microstrip–slotline tee junction with minimum size slotline terminations to reduce radiation loss. A multisection impedance transformation network is used to increase the operating bandwidth and minimize the parasitic coupling around the microstrip–slotline tee junction. As a result, the improved magic-T has greater bandwidth and lower phase imbalance at the sum and difference ports than the earlier magic-T design. The experimental results show that the 10-GHz magic-T provides more than 70% of 1-dB operating bandwidth with the average in-band insertion loss of less than 0.6 dB. It also has phase and amplitude imbalance of less than $\pm 1^\circ$ and ± 0.25 dB, respectively.**

***Index Terms*—Microstrip circuits, passive circuits, power combiners, power dividers, slotline transitions.**

I. Introduction

A MAGIC-T is a four-port junction. In an ideal case, it is lossless and has a sum (H) port and a difference (E) port that allow incident signals from ports 1 and 2 to be combined or subtracted with a well-defined relative phase (see Fig. 1). Structures approximating these ideal properties have been widely used as an element in correlation receivers, frequency discriminators, balanced mixers, four-port circulators, microwave impedance bridges, reflectometers [1], etc.

A magic-T requires components that are less dependent on transmission phase delay to perform as in-phase and out-of-phase combiners. Structures with high physical symmetry are often used in the magic-T design to produce broadband response with low phase and amplitude imbalance. Symmetry at the H port is simple to obtain using microstrip line [2] or coplanar waveguide (CPW) [3], whereas symmetry at the port E is simple to implement using slotline [4] or mode-conversion techniques using slotline structures [4]–[7].

On the other hand, magic-Ts with no physical symmetry at ports H or E require coupled lines [8] or left-handed elements [9] to compensate for phase variations. These magic-Ts can produce broadband response with some tradeoffs in high phase imbalance.

Manuscript received April 15, 2007; revised August 28, 2007.

K. U-yen and E. J. Wollack are with the NASA Goddard Space Flight Center, Greenbelt, MD 20771 USA (e-mail: kuyen@pop500.gsfc.nasa.gov).

J. Papapolymerou and J. Laskar are with the Department of Electrical and Computer Engineering, Georgia Institute of Technology, Atlanta, GA 22305 USA (e-mail: papapol@ece.gatech.edu).

Color versions of one or more of the figures in this paper are available online at http://ieeexplore.ieee.org.

Digital Object Identifier 10.1109/TMTT.2007.912213

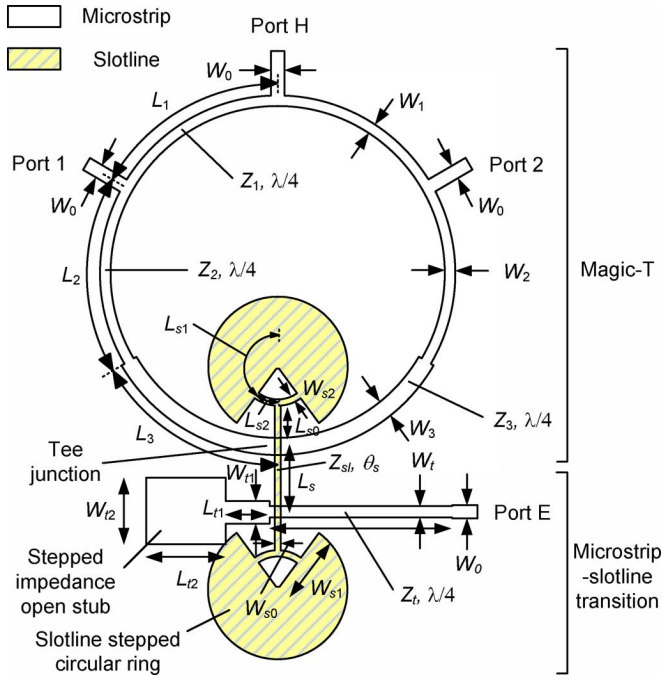

Fig. 1. Improved broadband magic-T using microstrip-to-slotline transitions.

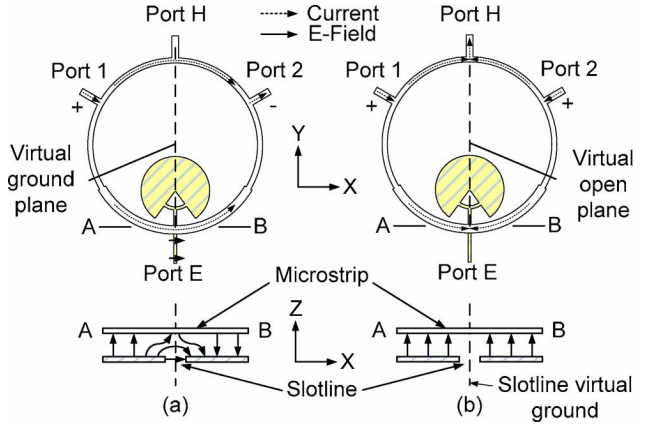

Fig. 2. (a) Odd- and (b) even-mode electric field and current flow in the magic-T and in the microstrip–slotline tee junction at A–B.

Although the symmetric magic-Ts using the slotline structure have a broadband power-combining response, their insertion loss, return loss, size, and fabrication complexity can limit their usefulness. The total slotline area in these magic-Ts can be large and susceptible to slotline radiation, which results in high

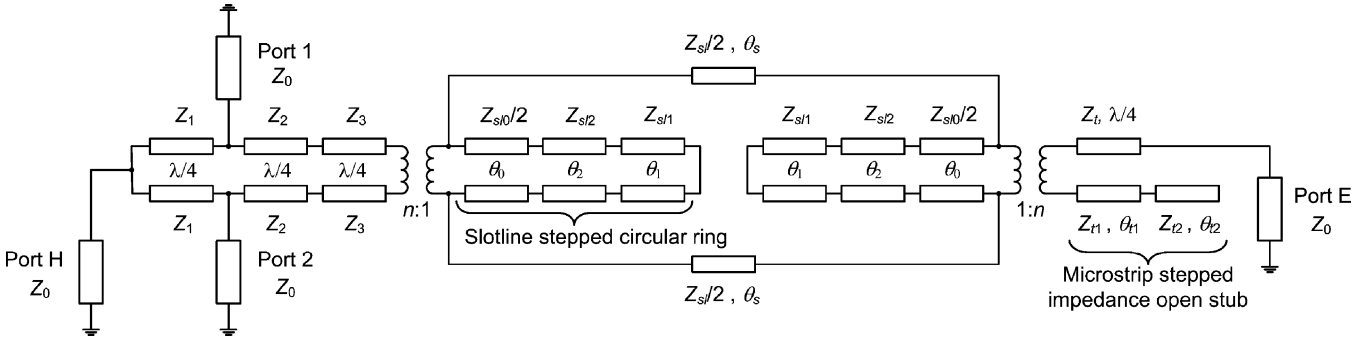

Fig. 3. Full circuit model of the magic-T at the center of the operating frequency.

insertion loss. In addition, magic-Ts using CPW–slotline transition require air bridges to prevent the excitation of undesired modes, which result in additional fabrication steps.

The previously proposed magic-T using microstrip–slotline transitions [7] produces a broad in-phase combining bandwidth using a small slotline area to minimize in-band loss. However, it has a narrowband port 1–2 isolation and port E–E return-loss response. In addition, it is sensitive to microstrip and slotline misalignment. This is due to: 1) the limited number of sections of quarter-wavelength ($\lambda/4$) impedance transformers used to match all four ports and 2) the strong parasitic couplings presented at the microstrip–slotline tee junction where four microstrip lines and a slotline are combined. The improved broadband magic-T design, discussed in this paper, introduces the new microstrip ring structure that minimizes parasitic couplings at the microstrip–slotline tee junction, and simultaneously enhances the return loss at ports 1, 2, and E and results in a small phase mismatch. The optimal design of the new structure also increases the overall bandwidth significantly.

II. Circuit Configuration

The improved structure, as shown in Fig. 1, consists of two sections, namely, a magic-T and a compact microstrip–slotline transition. The microstrip–slotline transition section has been studied in [7] and [10]. This paper focuses on the new approach in designing the magic-T section to simultaneously realize broadband return loss and isolation. The full magic-T transmission line model is also introduced. In addition, the practical upper limit of the magic-T operating bandwidth, designed following this approach, is derived.

The magic-T section in Fig. 1 consists of quarter-wavelength ($\lambda/4$) microstrip lines connected in a ring configuration. The top section of the ring, above ports 1 and 2, consists of two $\lambda/4$ lines with the characteristic impedance of Z_1. It is used as an in-phase combiner with the output port H between two Z_1 lines. The bottom section of the ring contains two pairs of $\lambda/4$ lines. Each pair contains two microstrip lines with the characteristic impedances of Z_2 and Z_3 connected in series. These lines are used to transform the microstrip to the slotline with the characteristic impedance of $Z_{\rm sl}$, and produce the microstrip–slotline tee junction at the center of the structure. The $Z_{\rm sl}$ line is terminated with two slotline stepped circular rings (SCRs) at both ends [10] to provide broadband virtual open. Finally, the slotline output is transformed to a microstrip output at port E using a microstrip–slotline transition. The magic-T is analyzed in both odd and even modes up to the slotline $Z_{\rm sl}$ section, as shown in Fig. 2(a) and (b), respectively.

In the odd mode, the signals from ports 1 and 2 are out-of-phase. This creates a microstrip virtual ground plane along the Y-axis of the magic-T and at port H, as shown in Fig. 2(a). The slotline SCR termination connected to the slotline $Z_{\rm sl}$ allows microstrip-to-slotline mode conversion to occur as indicated by electric field and current directions around the cross section A–B.

In the even mode, the signals from ports 1 and 2 are in-phase, thus creating a microstrip virtual open along the Y-axis of the magic-T, as shown in Fig. 2(b). Electric fields in the slotline at cross section A–B are canceled, thus creating a slotline virtual ground that prevents the signal flow to or from port E by symmetry.

A. Magic-T Circuit Model

The magic-T can be studied using the odd- and even-mode circuit analysis [7]. By using this analysis and ignoring parasitic reactance due to step in linewidth, we construct the full circuit model, as shown in Fig. 3. This model approximates the magic-T's response around the center frequency f_0.

In the odd mode, port H becomes a virtual ground. Using a $\lambda/4$ transformation through the Z_1 line, the virtual ground becomes an open at ports 1 and 2, both of which have a characteristic impedance of Z_0. To match the impedance at these ports, $\lambda/4$ transmission lines—Z_2 and Z_3—are used to transform Z_0 to the slot line impedance of $n^2 Z_{\rm sl}/2$, where n is the microstrip–slotline transformer ratio. In the single-mode limit, n is dependent on the substrate thickness, the transmission line characteristic impedance, and the microstrip–slotline physical alignment [11]. The general equation relating Z_0, Z_2, Z_3, and $Z_{\rm sl}$ can be expressed at f_0 as follows:

$$Z_0 = n^2 \frac{Z_{\rm sl}}{2} \left(\frac{Z_2}{Z_3} \right)^2. \tag{1}$$

It is desirable that $n^2 Z_{\rm sl}/2$ equals Z_0 to eliminate the discontinuity of microstrip lines (i.e., $Z_2 = Z_3$). However, in the fabrication process, typically the value $Z_{\rm sl}$ is limited by the allowable minimum slot width and substrate thickness. To minimize the radiation loss of the transition, we employ the minimum achievable slotline width ($W_{\rm sl}$) of 0.1 mm on the 0.25-mm-thick Roger's Duroid 6010 substrate. This slotline width corresponds to a $Z_{\rm sl}$ magnitude of 72.8 Ω.

TABLE I
CIRCUIT PARAMETERS AT 10 GHz USED IN THE MAGIC-T DESIGN ON 0.25-mm-THICK ROGER'S DUROID 6010 SUBSTRATE

Magic-T section		microstrip-slotline transitions
(a) General solution	Z_0=50 Ω, Z_1=70.7 Ω, Z_2=50 Ω, Z_3=42.7 Ω	Z_{t1}=40 Ω, Z_{t2}=20 Ω, Z_t=60.3 Ω, θ_1=24°, θ_2=48°, Z_{sl}=72.8 Ω,
(b) Optimized solution	Z_0=50 Ω, Z_1=57.52 Ω, Z_2=58.9 Ω, Z_3=47.7 Ω	Z_{sl0}=72.8 Ω, Z_{sl2}=72.8 Ω, Z_{sl1}=163.4 Ω, θ_s=31°, n=1, θ_0=14°, θ_1=34.95°, θ_2=6.2°

In the even mode, port E becomes a virtual open and it is half-wavelength transformed to an open at ports 1 and 2. Therefore, there is no constraint on the values Z_2 and Z_3 in this mode at f_0. Moreover, ports 1's and 2's impedances are transformed to $2Z_0$ at port H using the Z_1 line. The general solution can be obtained as follows:

$$Z_1 = \sqrt{2}Z_0. \tag{2}$$

B. Microstrip and Slotline Transition Terminations

The microstrip–slotline transition in the magic-T requires proper terminations to maintain broad mode conversion at the microstrip–slotline tee junction and at port E. The slotline SCR and the microstrip stepped-impedance open-stub terminations are used here due to its broadband characteristics. In addition, the slotline SCR is more compact and has lower radiation loss than many conventional slotline terminations.

The slotline SCR is modeled using three transmission lines $Z_{\rm sl0}$, $Z_{\rm sl1}$, and $Z_{\rm sl2}$ with electrical lengths of θ_0, θ_1, and θ_2, respectively [10]. These values correspond to the physical widths and lengths of W_{s0}, W_{s1}, and W_{s2}, and L_{s0}, L_{s1}, and L_{s2}, respectively.

The microstrip stepped-impedance open stub is modeled using two transmission lines Z_{t1} and Z_{t2} with electrical lengths of θ_{t1} and θ_{t2}, respectively. These values correspond to the physical widths and lengths of W_{t1} and W_{t2}, and L_{t1} and L_{t2}, respectively. The termination models shown in Fig. 3 can be used to accurately determine their frequency responses [10] with the circuit parameter values provided in Table I.

C. Magic-T's Optimal Parameter Values

The general solution based on (1) and (2) is used to construct the magic-T. Using the parameters in Table I(a), the magic-T provides broadband port E–E return loss and broadband port 1-E transmission, as shown in Fig. 4(a) and (b). However port 1-H2–H transmission and port 1–2 isolation have narrowband response due to all transmission poles being in line at f_0. To increase the return loss and isolation bandwidth of the magic-T, Z_1, Z_2, and Z_3 values can be numerically optimized using a circuit simulation software such that the microstrip linewidth step discontinuity is more gradual and the port 1-H/2–H transmission has equal-ripple response. The optimization goal is set to obtain the minimum port H–H return loss and port 1–2 isolation of 14 and 18 dB, respectively, over 70% bandwidth. The frequency responses of the magic-T using the optimized parameters in Table I(b) are shown in Fig. 4(a) and (b). The maximum

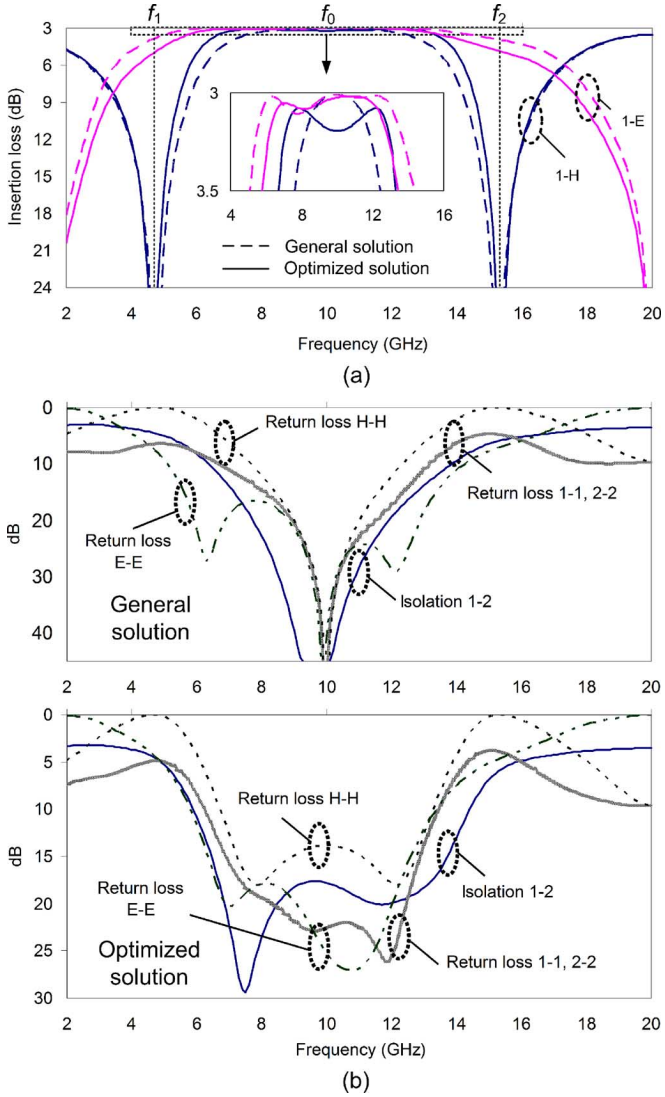

Fig. 4. Magic-T frequency responses of: (a) insertion loss and (b) return loss and isolation based on the circuit model shown in Fig. 4 and using the general and optimized solutions provided in Table I. $f_0 = 10$ GHz.

port 1-H and 2-H transmission bandwidth of the magic-T is limited by strong transmission zeros. These transmission zeros are due to the sections Z_2 and Z_3 as they transform a virtual open at the tee junction to a virtual ground at ports 1 and 2 in the even mode. This is shown in Fig. 4(a) at frequencies f_1 and f_2. Using (3) with $Z_2 = 58.9\ \Omega$ and $Z_3 = 47.7\ \Omega$, we find that f_1 and f_2 are $0.47f_0$ and $1.53f_0$, respectively. The upper port 1-E and 2-E transmission frequency band is

$$\frac{f_1}{f_0} = \frac{2}{\pi}\tan^{-1}\left(\sqrt{\frac{Z_3}{Z_2}}\right) = 2 - \frac{f_2}{f_0} \tag{3}$$

limited by the Z_1 section that creates transmission zero at $2f_0$ in the odd mode since it transforms a virtual ground at port H to a virtual open at ports 1 or 2. The lower port 1-E and 2-E transmission frequency band is limited by the microstrip–slotline transition and tee junction since the slotline SCR termination size becomes so small compared to the slotline wavelength that the slotline SCR effectively becomes a short.

TABLE II
PHYSICAL PARAMETERS IN MILLIMETERS OF THE MAGIC-T ON 0.25-mm-THICK ROGER'S DUROID 6010 SUBSTRATE

Microstrip line sections	Slotline sections
W_0=0.238, W_1=0.175, W_2=0.165, W_t=0.16, L_1=2.92, L_2=2.90, L_3=2.87, L_t=2.79 ,L_{t1}=0.68, W_{t1}=0.37, L_{t2}=1.30, W_{t2}=1.05	L_s=1.0, W_{sl}=0.10, L_{s0}=0.58, W_{s0}=0.10, L_{s1}=0.91, W_{s1}=0.71, L_{s2}=0.23, W_{s2}=0.1

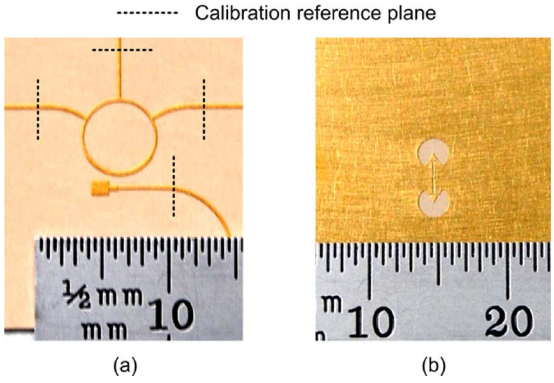

Fig. 5. (a) Top and (b) the bottom views of the improved magic-T.

III. HARDWARE DESIGN AND IMPLEMENTATION

A prototype magic-T was fabricated on a 0.25-mm-thick Rogers' Duroid 6010 substrate. The design uses the optimized solution presented in Table I(b) and the corresponding physical parameters of this design are shown in Table II. f_0 is set at 10 GHz. L_s is set to 1.0 mm to minimize slotline radiation loss while obtaining acceptable isolation between the microstrip line at port E and the microstrip–slotline tee junction. Z_{s1} is transformed to Z_0 at port E using a $\lambda/4$-long line with an impedance value of Z_t.

The photographs of the microstrip and slotline sections of the fabricated magic-T are shown in Fig. 5(a) and (b), respectively. The magic-T is connectorized and calibrated using the thru-reflect-line method with the reference plane shown in Fig. 5(a) and measured using a Hewlett-Packard 8510C network analyzer. Two magic-T ports are measured at a time while the other ports are terminated with 50-Ω broadband precision loads. The magic-T provides an average in-band insertion loss of 0.3 and 0.6 dB in the in-phase and out-of-phase power combining sections, respectively, as shown in Fig. 6(a). The 1-dB corner frequencies of the 1-H and 2-H transmissions are at 6.6 to 13.6 GHz and the in-band return loss of the magic-T is greater than 10 dB, as shown in Fig. 6(b). These measurements are in good agreement with the electromagnetic (EM) simulations and the circuit response predicted in Fig. 4(a) and (b). The 3-dB out-of-phase power combining section has higher insertion loss than the 3-dB in-phase combining section due to additional losses arising from the slotline radiation and microstrip line. The port E–H isolation is more than 32 dB, as shown in Fig. 7. The limit in the port E–H isolation at low frequency is mainly due to the finite conductivity and the area of ground plane that results in coupling leakage at the microstrip–slotline tee junction. In addition, the amplitude and

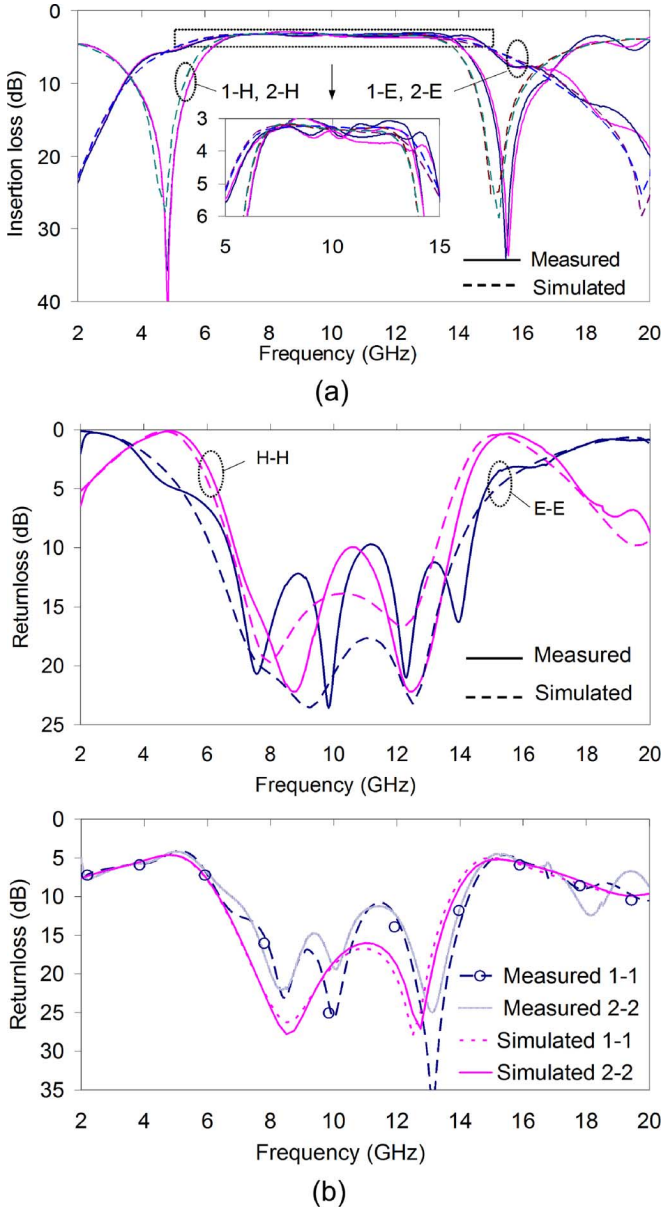

Fig. 6. Measured frequency responses of the: (a) insertion loss and (b) return loss of the optimized magic-T.

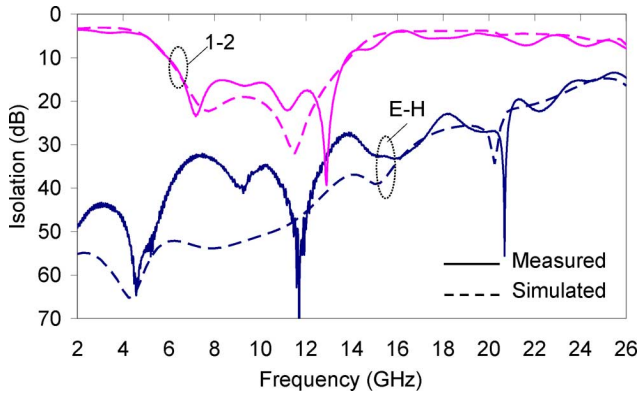

Fig. 7. Measured and simulated isolation at ports 1 and 2 and at port E–H of the magic-T.

the phase imbalance of the magic-T is less than ±0.25 dB and ±1°, as shown in Fig. 8(a) and (b), respectively. Transmission

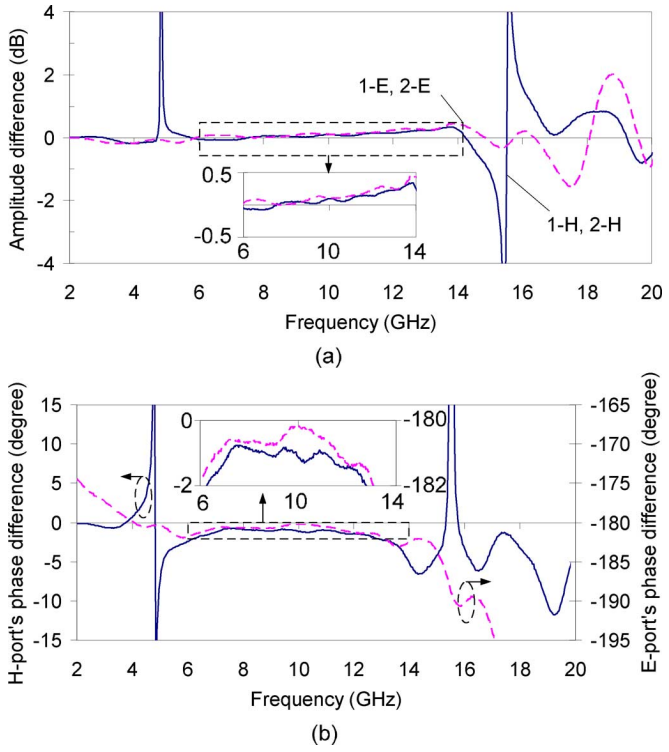

Fig. 8. Measured frequency responses of the: (a) amplitude imbalance and (b) phase imbalance of the optimized magic-T.

TABLE III
SUMMARY OF MEASURED PERFORMANCE OVER 1-dB INSERTION-LOSS BANDWIDTH OF THE MAGIC-T COMPARED WITH THE PRIOR MAGIC-T

	This work	Previous work [7]
Insertion loss (dB)	<0.6	<0.3
1-dB insertion loss bandwidth	75 %	24 %
Phase imbalance	±1 degree	±1.6 degree
Amplitude imbalance (dB)	±0.25	±0.3
Port 1-2 isolation (dB)	>15	>20
Port *E*-*H* isolation (dB)	>32	>31

zeros in the magic-T in the port 1-H and 2-H transmissions result in a sharp increase in-phase and amplitude imbalance at $f_1 = 4.76$ GHz and $f_2 = 15.5$ GHz. These frequencies are in agreement with those computed using (3). The measurement errors are dominated by the return-loss phase and amplitude mismatch at the connectorized broadband load terminations. A secondary error results from the bend line at port E, which results in perturbation in the phase and impedance mismatch at the reference plane. When compared with the previous design, this magic-T shows significant improvement in bandwidth. The magic-T also has less parasitic around the tee junction, which makes it less sensitive to fabrication misalignment. This results in a much smaller phase imbalance in this design. Their performance comparison is shown in Table III.

ACKNOWLEDGMENT

The authors would like to thank the Georgia Electronic Design Center, Georgia Institute of Technology, Atlanta, for providing microwave test facilities.

REFERENCES

[1] C. G. Montgomery, R. H. Dicke, and E. M. Purcell, *Principles of Microwave Circuits*, ser. MIT Rad. Lab. New York: McGraw-Hill, 1948, vol. 8, ch. 9–12.
[2] K. S. Ang and Y. C. Leong, "Converting balun into broadband impedance-transforming 180° hybrid," *IEEE Trans. Microw. Theory Tech.*, vol. 50, no. 8, pp. 1990–1995, Aug. 2002.
[3] L. Fan, C.-H. Ho, S. Kanamaluru, and K. Chang, "Wide-band reduced-size uniplanar magic-T, hybrid-ring, and de Ronde's CPW slot couplers," *IEEE Trans. Microw. Theory Tech.*, vol. 43, no. 12, pp. 2749–2758, Dec. 1995.
[4] J. P. Kim and W. S. Park, "Novel configurations of planar multilayer magic-T using microstrip–slotline transitions," *IEEE Trans. Microw. Theory Tech.*, vol. 50, no. 7, pp. 1683–1688, Jul. 2002.
[5] M. Aikawa and H. Ogawa, "A new MIC magic-T using coupled slot lines," *IEEE Trans. Microw. Theory Tech.*, vol. MTT-28, no. 12, pp. 523–528, Dec. 1980.
[6] G. J. Laughlin, "A new impedance-matched wideband balun and magic tee," *IEEE Trans. Microw. Theory Tech.*, vol. MTT-24, no. 3, pp. 135–141, Mar. 1976.
[7] K. U-yen, E. J. Wollack, J. Papapolymerou, and J. Laskar, "Compact planar magic-T using microstrip–slotline transition," in *IEEE MTT-S Int. Microw. Symp. Dig.*, Honolulu, HI, Jun. 2007, pp. 37–40.
[8] M. Arain and N. W. Spencer, "Tapered asymmetric magic tee," *IEEE Trans. Microw. Theory Tech.*, vol. MTT-23, no. 12, pp. 1064–1067, Dec. 1975.
[9] H. Okabe, C. Caloz, and T. Itoh, "A compact enhanced-bandwidth hybrid ring using an artificial lumped-element left-handed transmission line section," *IEEE Trans. Microw. Theory Tech.*, vol. 50, no. 3, pp. 798–840, Mar. 2004.
[10] K. U-yen, E. J. Wollack, S. Horst, T. Doiron, J. Papapolymerou, and J. Laskar, "Slotline stepped circular rings for low-loss microstrip-to-slotline transitions," *IEEE Microw. Wireless Compon. Lett.*, vol. 17, no. 2, pp. 100–102, Feb. 2006.
[11] J. P. Kim and W. S. Park, "Analysis of an inclined microstrip–slotline transition with the use of the spectral-domain immittance approach," *Microw. Opt. Technol. Lett.*, vol. 15, no. 4, pp. 256–260, Jul. 1997.

Kongpop U-yen (S'02–M'06) received the B.S. degree in electrical engineering from Chulalongkorn University, Bangkok, Thailand, in 1999, and the M.S. and Ph.D. degrees in electrical engineering from the Georgia Institute of Technology, Atlanta, in 2002 and 2006, respectively.

In 2000, he was an Engineer with L3 Communications, San Diego, CA, in 2000, where he was responsible for several switching power supply design. In 2001, he joined Texas Instruments Incorporated, where he designed BiCMOS integrated-circuit RF transmitters. In 2004, he joined the NASA Goddard Space Flight Center, Greenbelt, MD, where he is currently a Senior Design Engineer. His research interests are millimeter-wave passive components and RF integrated-circuit designs.

Edward J. Wollack (S'85–M'87–SM'98) received the B.Sc. degree in physics (with a math minor) from the Institute of Technology, University of Minnesota at Minneapolis, in 1987, and the M.Sc. and D.Sc. degrees in physics from Princeton University, Princeton, NJ, in 1991 and 1994, respectively.

In 1994, he began a post-doctoral fellowship with the Central Development Laboratory, National Radio Astronomy Observatory, Charlottesville, VA, with a concentration on low-noise millimeter-wavelength detectors and receiver systems for precision continuum radiometry. In 1998, he joined the Laboratory for Astronomy and Solar Physics, NASA Goddard Space Flight Center, Greenbelt, MD, where he is currently an Astrophysicist. His research interests include astrophysical and remote sensing, radiometric measurement and calibration techniques, and device noise theory.

John Papapolymerou (S'90–M'99–SM'04) received the B.S.E.E. degree from the National Technical University of Athens, Athens, Greece, in 1993, and the M.S.E.E. and Ph.D. degrees from The University of Michigan at Ann Arbor, in 1994 and 1999, respectively.

From 1999 to 2001, he was an Assistant Professor with the Department of Electrical and Computer Engineering, University of Arizona, Tucson. During the summers of 2000 and 2003, he was a Visiting Professor with the University of Limoges, Limoges, France. From 2001 to 2005, he was an Assistant Professor with the School of Electrical and Computer Engineering, Georgia Institute of Technology, Atlanta, where he is currently an Associate Professor. He has authored or coauthored over 140 publications in peer-reviewed journals and conferences. His research interests include the implementation of micromachining techniques and microelectromechanical systems (MEMS) devices in microwave, millimeter-wave and terahertz circuits and the development of both passive and active planar circuits on semiconductor (Si/SiGe, GaAs) and organic substrates [liquid-crystal polymer (LCP), low-temperature co-fired ceramic (LTCC)] for system-on-a-chip (SOC)/system-on-package (SOP) RF front ends.

Dr. Papapolymerou is the vice-chair for Commission D of the U.S. National Committee of URSI. He is an associate editor for IEEE MICROWAVE AND WIRELESS COMPONENT LETTERS and the IEEE TRANSACTIONS ON ANTENNAS AND PROPAGATION. During 2004, he was the chair of the IEEE Microwave Theory and Techniques (MTT)/Antennas and Propagation (AP) Atlanta Chapter. He was the recipient of the 2004 Army Research Office (ARO) Young Investigator Award, the 2002 National Science Foundation (NSF) CAREER Award, the Best Paper Award presented at the 3rd IEEE International Conference on Microwave and Millimeter-Wave Technology (ICMMT2002), Beijing, China, and the 1997 Outstanding Graduate Student Instructional Assistant Award presented by the American Society for Engineering Education (ASEE), The University of Michigan at Ann Arbor Chapter. His student was also the recipient of the Best Student Paper Award presented at the 2004 IEEE Topical Meeting on Silicon Monolithic Integrated Circuits in RF Systems, Atlanta, GA.

Joy Laskar (S'84–M'85–SM'02–F'05) received the B.S. degree in computer engineering (with math/physics minors) from Clemson University, Clemson, SC, in 1985, and the M.S. and Ph.D. degrees in electrical engineering from the University of Illinois at Urbana-Champaign, in 1989 and 1991, respectively.

Prior to joining the Georgia Institute of Technology, Atlanta, in 1995, he has held faculty positions with the University of Illinois at Urbana-Champaign and the University of Hawaii. With the Georgia Institute of Technology, he holds the Joseph M. Pettit Professorship of Electronics and is currently the Chair for the Electronic Design and Applications Technical Interest Group, the Director of Georgia's Electronic Design Center, and the System Research Leader for the National Science Foundation (NSF) Packaging Research Center. He heads a research group with a focus on integration of high-frequency electronics with opto-electronics and integration of mixed technologies for next-generation wireless and opto-electronic systems. His research has focused on high-frequency integrated-circuit design and their integration.